

# Assimilation of Satellite-derived Aerosol Optical Thickness and Online Integration of Aerosol Radiative Effects in a Mesoscale Model

Jun Wang\*, U. S. Nair, and Sundar A. Christopher

Department of Atmospheric Sciences  
University of Alabama in Huntsville, Huntsville, AL, 35805

## Abstract

To investigate the importance of aerosol radiative effect in the atmosphere, numerical simulation of a dust event during the Puerto Rico Dust Experiment (PRIDE) is presented by using the Colorado State University (CSU) Regional Atmospheric Modeling System (RAMS). Through assimilation of aerosol optical thickness (AOT) retrieved from a geostationary satellite, spatial and temporal aerosol distribution is optimally characterized during the simulation, which facilitates the accurate estimation of aerosol radiative effects. Radiative effect of dust aerosols is considered using different types of radiative transfer. Comparisons against observations show that a direct online consideration of aerosol radiative effects produces the best results. Numerical simulations show that for the atmospheric dust loading considered in this study, the uncertainty in the simulated AOT is 0.05 (10%) and the surface energy balance is different by  $40 \sim 60 \text{ Wm}^{-2}$  if the aerosol radiative effects are not properly represented. The dust radiative effect on the 2m air temperature and atmospheric heating rate are quantitatively analyzed. The results from this study demonstrate that the assimilation of satellite aerosol retrievals not only improves the aerosol forecasts but also has the potential to reduce the uncertainties in modeling the surface energy budget and other associated atmospheric processes.

## 1 Introduction

Dust aerosols, which are prevalent over the desert, can be transported to downwind areas thousands of kilometers away from source regions [Prospero, 1999], degrading visibility and air quality, perturbing the radiative transfer in the atmosphere [Carlson and Benjamin, 1980], providing a vector for disease causing organisms [Shinn *et al.*, 2000], and exacerbating symptoms in people with asthma [Prospero, 1999]. On the other hand, the atmospheric deposition of dust aerosols containing iron and other trace elements is an important nutrient source for the oceanic biota [Duce, 1991]. Both satellite remote sensing and numerical models have been used to study dust radiative effects [Christopher *et al.*, 2003] and to monitor dust transport [Wang and Christopher, 2003].

Satellite remote sensing data sets are widely used to map the geographical distribution of aerosols at high spatial and temporal resolutions and to explore the bulk effects of atmospheric aerosols on the earth's radiation budget. However, numerical mod-

els are the preferred tool for studying the role of tropospheric aerosols in modulating several important atmospheric processes such as surface energetics and atmospheric heating rates [Carlson and Benjamin, 1980]. Currently, satellite-derived aerosol information is not commonly used in numerical models, especially regional models. Using a case study of a dust event observed during the Puerto Rico Dust Experiment (PRIDE, [Reid *et al.*, 2003]), we explore the utility of assimilating satellite derived aerosol information into numerical models, to study aerosol radiative effects and address the following questions:

- Will aerosol retrievals from geostationary satellites with high temporal resolution provide an opportunity for the short-term aerosol forecast?
- Will online consideration of (atmosphere response or feedbacks to) the aerosol radiative effects give a better simulation of aerosols?

## 2 Data and the Area of Study

The area of study (Figure 1) is centered on Puerto Rico which was also the base for the PRIDE.

\*Email: wangjun@nssstc.uah.edu

Of the five major dust events that were recorded during PRIDE [Reid *et al.*, 2003], we study the most severe event that occurred during July 19th ~ July 23rd, 2000. Profiles of aerosol concentration from aircraft measurements, longwave and shortwave downwelling radiative flux ( $\text{Wm}^{-2}$ ) data from Surface Measurements for Atmospheric Radiative Transfer (SMART) [Ji and Tsay, 2000], Sunphotometer inferred Aerosol Optical thickness (AOT), and 2-m air temperature measurements made during PRIDE, are used. The location of two Sunphotometers are shown in Figure 1 including Roosevelt Road (RR, 18.20 N, 65.60 W), and La Paguera (LP, 17.97 N, 67.05 W). However, for this study, only AOT at LP is used, since data at RR during July 19th ~ July 23rd were not available. Further details regarding the data sets can be found in [Reid *et al.*, 2003]. During PRIDE, dust AOTs retrieved from the GOES 8 imager [Wang *et al.*, 2003] are used for studying the diurnal change of dust forcing at the top of atmosphere (TOA) and at the surface [Christopher *et al.*, 2003]. The GOES 8 AOTs compare well with in situ and ground-based Sunphotometer measurements [Wang *et al.*, 2003] and therefore are assimilated into the RAMS to model the dust transport. The National Center for Environmental Prediction (NCEP) reanalysis atmospheric data [Kalnay *et al.*, 1996] from 0, 6, 12 and 18 UTC, are used as a first guess for creating analysis of the meteorological fields used for specifying the initial conditions of the numerical model and for the evolution of the lateral boundary conditions during the simulation.

### 3 Methodology

The CSU RAMS (Version 4.3) [Cotton *et al.*, 2002; Pielke *et al.*, 1992], is modified to assimilate the AOTs retrieved from GOES 8 during the PRIDE time period [Wang *et al.*, 2003]. Currently the RAMS does not have a radiative transfer method that accounts for aerosol effects such as dust. Therefore, the RAMS was modified to include a sophisticated  $\delta$ -four-stream radiative transfer model (hereafter,  $\delta$ -4S RTM, [Liou *et al.*, 1988; Fu and Liou, 1993]) that includes dust aerosol properties measured during PRIDE [Christopher *et al.*, 2003]. The aerosol transport model is built upon a tracer advection module in RAMS combined with additional specification of source and sink mechanisms.

#### 3.1 Radiative Transfer Models

The RAMS provides three options of varying sophistication for longwave and shortwave radiation

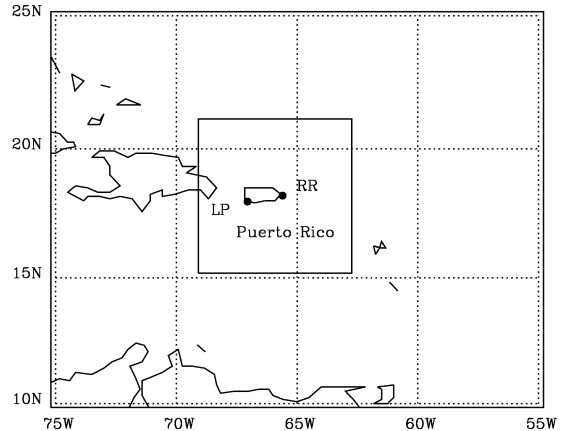


Figure 1: Model Domain. The inset rectangle shows the domain with fine grids. Also shown is the location of Roosevelt Road (RR, 18.20 N, 65.60 W), and La Paguera (LP, 17.97 N, 67.05 W) where the ground-based measurements are made routinely during PRIDE.

calculations. The first one developed by Mahrer and Pielke [1977] (hereafter Mahrer/Pielke scheme) is simple and efficient but it does not account for clouds. The second radiation method by Chen and Cotton [1983] (hereafter Chen/Cotton scheme) uses a two-stream model for solar radiation, and an emissivity approach for longwave radiation that accounts for radiative transfer in cloudy atmosphere but is computationally more expensive compared to the first technique. The third option utilizes a more sophisticated two-stream radiation scheme, that is able to treat the interaction of three solar and five infrared bands with detailed liquid water and ice hydrometeor size-spectra simulated from both bulk and bin-resolving microphysics models in RAMS [Harrington, 1997] (hereafter Harrington scheme). However, none of three existing radiation schemes in the RAMS accounts for the radiative interactions of aerosols. Hence, the  $\delta$ -4S RTM is implemented in the RAMS to compute the aerosol radiative effect online.

The  $\delta$ -4S RTM is a plane-parallel broadband radiative transfer model, originally designed to calculate the flux at TOA and surface in clear and cloudy conditions [Fu and Liou, 1993], and later was modified for calculation of radiative effect of aerosols such as dust [Christopher *et al.*, 2003; Liao and Seinfeld, 1998]. In this model, better representation of dust forward scattering for the flux calculations is achieved by using a  $\delta$  function [Liou *et al.*, 1988]. Our recent studies indicate an excellent agreement be-

tween calculated and observed downward shortwave irradiance at the surface, with differences of less than 3% when aerosol effects are carefully considered in the  $\delta$ -4S RTM calculations [Christopher *et al.*, 2003]. In this study, wavelength-dependent dust radiative properties in the shortwave spectrum derived from PRIDE [Wang *et al.*, 2003; Christopher *et al.*, 2003] and in the longwave spectrum from *d'Almeida et al.* [1991] are used.

### 3.2 Aerosol Model and Assimilation Method

The RAMS provides a generalized framework for advection and diffusion of three dimensional scalar quantities. In addition to scalar fields such as temperature and water vapor as routinely used in standard computations, the RAMS allows for specification of up to hundred additional scalars. Since the advection module including diffusion exchange of scalar variables is already available in RAMS, new emission/deposition parameterizations are then incorporated into the model to simulate the aerosol transport. During the PRIDE, dust and sea salt are the two major types of aerosols in the atmosphere [Reid *et al.*, 2003]. In this study, the sea salt concentrations is diagnosed as a function of wind speeds near the ocean surface [Collins *et al.*, 2001]. Since the majority of the large dust particles (diameter > 10  $\mu\text{m}$ ) is removed (deposited) during the dust transport from the Saharan desert to the Puerto Rico regions [Schtz and Jaenicke, 1974; Maring *et al.*, 2003], the vertical variations of the normalized dust size distribution usually is small during the dust event in PRIDE [Reid *et al.*, 2003]. This allows us to focus on the simulation of dust mass concentration in the model, and use constant dust optical properties (e.g., single scattering albedo, asymmetric factor and extinction coefficient) in radiative calculations. The dry deposition process is modeled using scheme by [Slinn and Slinn, 1980]. Wet deposition process is not included in the model simulation, because of cloud-free atmosphere and no precipitation recorded during the study time period .

GOES 8 AOT is assimilated into the RAMS using the Newtonian nudging scheme in which the values of model predicted AOT tendency are adjusted and modeled AOT are relaxed towards the satellite retrieved AOT:

$$\left[\frac{\partial \tau'_{mod-dust}}{\partial t}\right]_t = (1 - \varepsilon) \left[\frac{\partial \tau_{mod-dust}}{\partial t}\right]_t + \frac{\varepsilon [\tau_{GOES}]_{t+1} - [\tau_{mod-salt} + \tau_{mod-dust}]_t}{\delta \times \Delta t} \quad (1)$$

In the above equation, the left side is the updated tendency of simulated dust AOT for the time step  $t$  after the assimilation. The first term on the right is the tendency of dust AOT at time step  $t$  before the assimilation, and  $\tau_{mod-salt}$  is the optical thickness of sea salt. The GOES 8 AOT at time step  $t+1$  (e.g.,  $[\tau_{GOES}]_{t+1}$ ) is computed by linear interpolation of GOES 8 AOT from the two assimilation time periods. The difference between  $[\tau_{GOES}]_{t+1}$  and the simulated AOT (sum of mod-salt and mod-dust) at time step  $t$  divided by the integration time interval  $\Delta t$  is the time tendency if we want to force the modeled AOT to match the GOES 8 AOT in the time step  $t+1$  (recall  $\tau_{t+1} = \tau_t + tendency \times \Delta t$ ). This tendency is then adjusted by a confidence factor  $\delta$ , where smaller  $\delta$  (nearly equal to 1) implies that GOES 8 AOT has very high accuracy, hence larger confidence of this tendency term. The  $\varepsilon$  value in equation (1) is a 2D weighting factor which is used in RAMS to control the effect of the nudging term as a function of spatial location. Notice, for  $\delta = 1$  and  $\varepsilon = 1$ , the effect of the modeled AOT tendency will be neglected, and equation (1) forces the modeled AOT to exactly relax towards the GOES 8 AOT. We set  $\delta = 1.02$  after the considering that GOES 8 AOT has a slight overestimate bias [Wang *et al.*, 2003]. After the modeled AOT tendency is optimally modified (updated) from equation (1), the modeled dust concentration tendency in each layer is then adjusted by assuming the shape of aerosol vertical distribution is the same before and after the assimilation [Collins *et al.*, 2001]. A detailed description of the methodology used in this study can be found in Wang *et al.* [2004].

## 4 Model Configuration and Experiment Design

The numerical simulation in this study utilizes a nested grid configuration; a fine grid of  $34 \times 34$  points and 40km grid spacing covering the island of Puerto Rico, nested within a coarse grid with  $32 \times 32$  grid points and 80km grid spacing (Figure 1). Both the configurations use a stretched vertical grid of 30 grid points and grid stretch ratio of 1.2, with the vertical grid spacing increasing from 100m near the surface to a maximum of 750m higher up in the atmosphere. To evaluate the dust radiative effects, four simulation experiments with different radiative transfer schemes and different treatment of aerosol radiative effects are conducted (Table 1). All simulations started at 12 UTC, July 20th 2000 and ended at 12 UTC on July 23rd of 2000. A time step of 60

Table 1: Model differences in four simulation cases

Case Name	Radiation Schemes Used	How aerosol radiative effect is treated
$\delta$ -4S-online	$\delta$ 4 Stream	Explicitly considers aerosol effects
Harrington	2 Stream	Does not consider any aerosol radiative effects
Mahrer/Pielke	Simple parameterization	Does not consider any aerosol radiative effects
$\delta$ -4S-off-line	$\delta$ 4 Stream	Does not consider any aerosol radiative effects

and 10 seconds are used for time stepping the coarse and fine grids, respectively. The GOES 8 AOT product has spatial resolution of  $4\text{km} \times 4\text{km}$  [Wang *et al.*, 2003]. Three dimensional aerosol concentration fields derived from GOES 8 data valid at 1200 UTC, July 20th 2000 are then averaged into 40km and 80km grids to initialize aerosol fields in the model. Although GOES 8 AOT has a temporal resolution of 30 minutes, the model only assimilates the GOES8 AOT twice per day, one at 1331 UTC, and one at 1931 UTC.

## 5 Results

Figure 2 showed the spatial distribution of modeled AOT with and without assimilation at several time periods. Also shown in Figure 2 is the corresponding GOES 8 AOT spatial distributions. Without nudging the boundary of modeled AOT to the GOES 8 AOT, the model can not define the dust source near the model boundary. In this case, as shown in Figure 2 B1-B2, dust layer moves quickly across the model domain, and disappears only in one day. This is a typical problem for a meso-scale model if the meso-scale model boundary is not updated for a longer period of time. Hence, the assimilation of GOES 8 provides a constrain to the model boundaries, and makes the simulation more realistic.

Comparison of modeled results with in situ measurements is shown in Figure 3. The modeled AOT matches the Sunphotometer AOT, and captures the temporal evolution of dust event very well (Figure 3a). Though the simple linear nudging technique (see equation 1) is used in this study, the nudging provides a correction for the dynamical simulations in the model. Such improvement is obvious, as the modeled AOT can capture the diurnal variations of AOT very well (Figure 3a), especially when the dust reached the Puerto Rico. The maximum difference of AOTs in four different numerical modeling simulations (Table 1) is approximately 0.05 and mainly occurs at midday hours (Figure 3a). Overall, the difference of AOTs in four simulations is within 10%

(the averaged AOT value is 0.45). The online  $\delta$ -4S-online simulation produces the best match with the Sunphotometer (SP) AOT.

Of the different radiative transfer parameterizations examined in this study, the Mahrer/Pielke scheme shows maximum deviation from the measured downwelling shortwave flux at the surface (Figure 3b), and the  $\delta$ -4S-online simulation shows the least. This is a common feature for most mesoscale models in which the downward shortwave flux is usually larger than the actual value, mainly because the aerosol scattering effect is neglected in the radiative transfer calculations (e.g., [Chen and Dudhia, 2001]). As in this study, such overestimation ranges from  $60\text{Wm}^{-2}$  to  $100\text{Wm}^{-2}$ , though specific values also depends on the radiative schemes, the magnitude of dust AOTs, and the simulation time (e.g., solar zenith angle; Figure 3b). Overall, the  $\delta$ -4S-online simulation has the best match with the observed downwelling shortwave fluxes.

Dust absorbs in the longwave part of the atmospheric radiation spectrum [d’Almeida *et al.*, 1991] and this effect is obvious when comparing the model simulated downwelling longwave flux with surface observations (Figure 3c). The dust layer absorbs the outgoing longwave flux from the surface, and re-emits it back to the surface. This process therefore increases the downward longwave flux. All four simulations underestimate the downward longwave fluxes (Figure 3c). But, because the  $\delta$ -4S-online explicitly considers the dust absorption, it shows the least deviation from the observations. Note that the simulated downwelling longwave flux represents an average over  $40\text{km} \times 40\text{km}$  area while observations are essentially point measurements and probably accounts for some of the differences. Compared to the  $\delta$ -4S-online simulation, all other simulations exhibit a “cool” bias (less downward longwave) at the surface (Figure 3d). The differences ranges from  $-60\text{Wm}^{-2}$  (Harrington scheme) to less than  $-10\text{Wm}^{-2}$  ( $\delta$ -4S-offline simulation).

The comparison of the total flux difference (shortwave plus longwave) is highly variable and depends on the radiative transfer scheme and the mag-

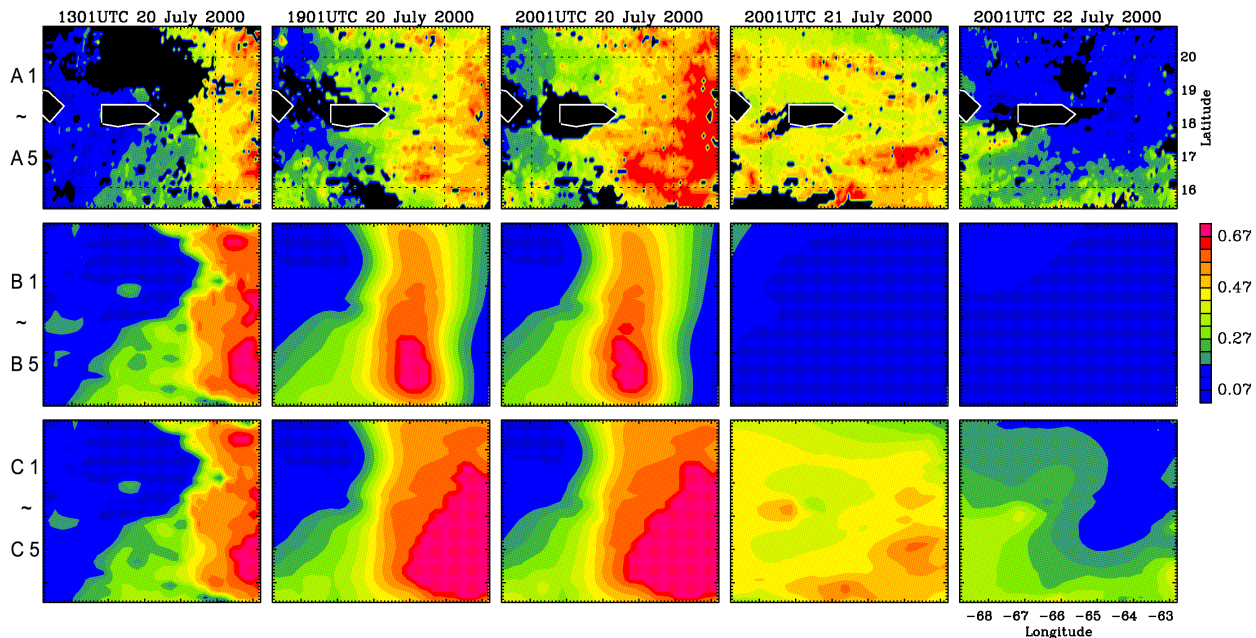


Figure 2: Spatial distribution of GOES 8 AOT (A1-A5, [Wang et al., 2003]) and RAMS simulated AOT without assimilation (B1-B5) and with assimilation (C1-C5).

nitude of AOT (figure not shown). Simulations conducted using the Mahrer/Pielke radiative transfer parameterization and the Harrington scheme exhibit positive bias during the daytime due to overestimation of incoming solar flux at the surface, and the negative bias during the night due to lack of consideration of re-emitted longwave flux from the dust layer. The least difference (compared to the  $\delta$ -4S-online) is the  $\delta$ -4S-offline simulation, where the radiative scheme is the same but the aerosol radiative effects are not explicitly considered. However, even in the offline case, a  $40 \text{ Wm}^{-2}$  difference still exists. Since downwelling fluxes are crucial inputs for the surface energy budgets, it is expected that  $\delta$ -4S-online simulation would have a better performance in modeling surface and 2m air temperature, as shown in Figure 3d. One interesting feature in Figure 3d is that  $\delta$ -4S-online captures a slight temperature decrease when the dust is over Puerto Rico resulting in the slight decrease of temperature in the noon time of July 21st 2000. On the third day of the simulations, the temperature in the Mahrer/Pielke case best match the observed temperature, while the other 3 cases all have a lower temperature. However note that the Mahrer/Pielke radiative transfer parameterization gives the right answer for the wrong reasons due to the significant overestimation of downwelling solar flux at the surface. The  $\delta$ -4S-online simulation on the other hand underesti-

mates the solar flux at the surface due to the simulated AOT being larger compared to the actual AOT (Figure 3a). Hence,  $\delta$ -4S-online simulation overestimates the aerosol scattering effects during the daytime, producing cooler temperatures while the  $\delta$ -4S-offline simulation, that does consider the aerosol effect, is significantly warmer. Due to the underestimation of downwelling longwave flux (Figure 3c), the simulated nocturnal temperature in four different simulations are all lower than the measurements (Figure 3d). Nocturnal temperature evolution in the  $\delta$ -4S-online simulation has the least bias compared to measurements, because it explicitly consider the dust absorption in the atmosphere which in turn emits more longwave flux back to the surface. The Mahrer/Pielke scheme seems to have a comparable performance as  $\delta$ -4S-online, but this is due to the overestimation of downward shortwave during the day balanced by the underestimation of downward longwave flux during both day and night. Overall, the  $\delta$ -4S-online simulation shows the best performance in modeling 2m air temperature.

Previous studies [Carlson and Benjamin, 1980; Haywood et al., 2001] showed that the radiative absorption by Saharan dust particles can enhance the atmospheric heating rate (typically more than  $1\text{K/day}$ ) over the Saharan regions. In this study, we found that the difference of the daily averaged atmospheric radiative heating rate in both  $\delta$ -4S-online

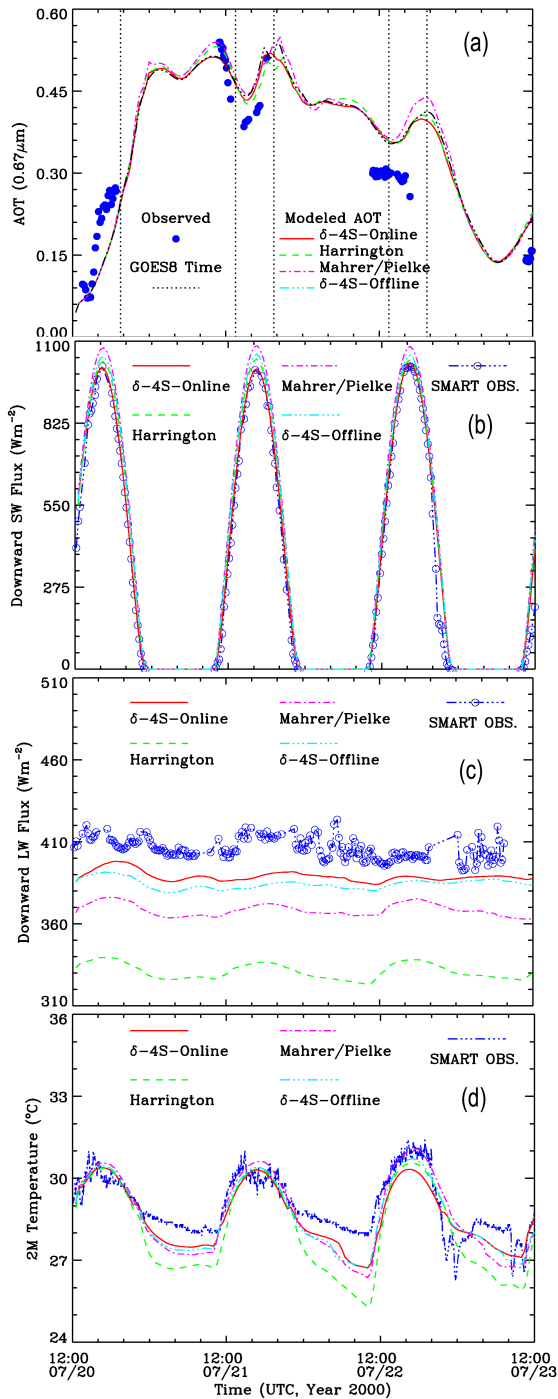


Figure 3: (a) Modeled AOT vs. Observed AOT at La Paguera. Vertical dotted lines show the time periods (1331UTC and 1991UTC on each day) when GOES AOTs are assimilated into the model. Comparisons between measured and modeled downwelling shortwave fluxes and longwave fluxes are shown in (b) and (c) respectively. (d) is similar as (b) but for the comparison of 2m air temperature

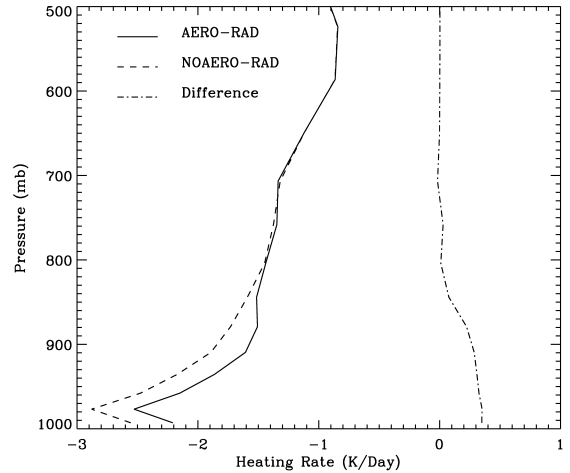


Figure 4: Daily (24 hrs) averaged atmospheric radiative (both longwave and shortwave) heating rate on July 21st 2000 over the ocean in a grid that is nearest to the La Paguera ( $17.97^{\circ}\text{N}$ ,  $67.05^{\circ}\text{W}$ ). AERO-RAD and NOAERO-RAD represent heating rate calculated in  $\delta$ -4S-online and  $\delta$ -4S-offline, respectively.

and  $\delta$ -4S-offline cases is nearly zero in the upper troposphere and becomes larger up to  $0.3\text{K/day}$  in the lower troposphere where the dust layer is located (Figure 4). The change of heating rate and the surface energy budget due to the dust radiative effect will then in turn change the wind fields and the dust spatial distribution, which is an important reason for the difference of the dust AOT simulated in  $\delta$ -4S-online and  $\delta$ -4S-offline cases. Hence,  $\delta$ -4S-online simulation that integrates the dust radiative effects during the simulation gives the best results when compared with in situ observations.

## 6 Summary and Discussion

A method for assimilating the satellite derived AOT into the regional mesoscale models is developed. By adding a  $\delta$ -4S RTM into the RAMS, the aerosol radiative effect on the surface energy budget and atmospheric radiative heating rate are examined through the different simulation experiments. Comparison with in situ measurements showed that the  $\delta$ -4S-online simulation that explicitly accounts for aerosol radiative effects best simulates the evolution of downwelling radiative fluxes at the surface as well as the 2m air temperature and radiative heating rate in the lower troposphere. Our results further showed that the simulated AOT could vary by up to 0.05 (10%) if aerosol radiative effects are ignored. This implies that inclusion of aerosol radiative

effect in the model are important not only for the surface energy budget and temperature modeling but also for the simulation of aerosol transport. Offline models without explicitly considering the aerosol radiative effects therefore may exhibit biases in modeling the aerosol transport. Such bias could be severe during the aerosol pollution events when larger aerosol radiative effects are expected. Future studies through assimilation of MODIS AOT and online consideration of atmosphere response to the aerosol radiative effect could narrow these uncertainties.

### Acknowledgements

This research was supported by NASA's Radiation Sciences, Interdisciplinary sciences and ACPMAP programs, NASA grant NAG5-11941 and National Science Foundation grant ATM-0128924. J. Wang was supported by NASA Earth System Sciences Fellowship program (ESSF/04-0000-0272). We're grateful to Drs. Jeffrey Reid (Naval Research Laboratory at Monterey, CA), Hal Maring (University of Miami), Brent N. Holben, Si-Chee Tsay and Qiang Ji (NASA Goddard Space Flight Center) for their PRIDE data sets. We also thank Mr. Deepak Ray for his help in the early stages of the model configuration.

### References

Carlson, T. N., and S. G. Benjamin, Radiative heating rate of Saharan dust, *J. Atmos. Sci.*, *37*, 193 - 213, 1980.

Chen, C., and W. R. Cotton, A one-dimensional simulation of the stratocumulus-capped mixed layer, *J. Atmos. Sci.*, *44*, 2951-2977, 1983.

Chen, F., and J. Dudhia, Coupling an advanced land surface-hydrology model with Penn State-NCAR MM5 modeling system. Part II: Preliminary model validation, *Mon. Wea. Rev.*, *129*, 587-604, 2001.

Christopher, S., J. Wang, Q. Ji, and S.-C. Tsay, Estimation of diurnal shortwave dust aerosol radiative forcing during PRIDE, *J. Geophys. Res.*, *108*, doi:10.1029/2002JD002787, 2003.

Collins, W. D., P. J. Rasch, B. E. Eaton, B. Khatatov, and C. S. Zender, Simulating aerosols using a chemical transport model with assimilation of satellite aerosol retrievals: Methodology for INDOEX, *J. Geophys. Res.*, *106*, 7313-7336, 2001.

Cotton, W., et al., RAMS 2001: Current status and future directions, *Meteorol. Atmos. Phys.*, pp. doi 10.1007/s00703-001-0584-9, 2002.

d'Almeida, G. A., P. Koepke, and E. P. Shettle, Atmospheric climatology and radiative characteristics, *A. Deepak publishing*, p561., 1991.

Duce, R., The atmospheric input of trace species to the world ocean, *Global Biogeochem. Cycles*, *5*, 193-259, 1991.

Fu, Q., and K. N. Liou, Parameterization of the radiative properties of cirrus clouds, *J. Atmos. Sci.*, *50*, 2008-2025, 1993.

Harrington, J. Y., The effects of radiative and microphysical processes on simulated warm and transition season Arctic stratus, Phd diss., Atmospheric Sciences Paper No. 637, Colorado State University, Fort Collins, CO 80523, 1997.

Haywood, J., P. N. Francis, M. D. Glew, and J. P. Taylor, Optical properties and direct radiative effect of Saharan dust: A case study of two Saharan dust outbreaks using aircraft data, *J. Geophys. Res.*, *106*, 18,417-18,430, 2001.

Ji, Q., and S.-C. Tsay, On the dome effect of Eppley pyrgeometers and pyranometers, *Geophys. Res. Lett.*, *27*, 971-974, 2000.

Kalnay, E., et al., The NCEP/NCAR 40-year reanalysis project, *Bullet. Amer. Meteorol. Soc.*, *77*, 437-471, 1996.

Liao, H., and J. Seinfeld, Radiative forcing by mineral dust aerosols: sensitivity to key variables, *J. Geophys. Res.*, *103*, 31,637-31,645, 1998.

Liou, K. N., Q. Fu, and T. P. Ackerman, A simple formulation of the d-four-stream approximation for radiative transfer parameterizations, *J. Atmos. Sci.*, *45*, 1940-1947, 1988.

Mahrer, Y., and R. Pielke, A numerical study of the air-flow over irregular terrain, *Beitrag zur Physik der Atmosphäre*, *50*, 98-113, 1977.

Maring, H., D. L. Savoie, M. A. Izaguirre, and L. Custals, Mineral dust aerosol size distribution change during atmospheric transport, *J. Geophys. Res.*, *108*, 8592, doi:10.1029/2002JD002536, 2003.

Pielke, R., R. L. Walko, J. Eastman, W. A. Lyons, R. A. Stocker, M. Uliasz, and C. J. Trempack, A comprehensive meteorological modeling system - RAMS, *Meteor. Atmos. Phys.*, *49*, 69-91, 1992.

Prospero, J., Long-term measurements of the transport of African minerals dust to the southeastern United States: implications for regional air quality, *J. Geophys. Res.*, pp. 15,917-15,927, 1999.

Reid, J. S., et al., Measurements of Saharan dust by airborne and ground-based remote sensing methods during the Puerto Rico Dust Experiment (PRIDE), *J. Geophys. Res.*, *108*, doi:10.1029/2002JD002493, 2003.

Schtz, L., and R. Jaenicke, Particle number and mass distribution above 10-4 cm radius in Sand and Aerosol of the Sahara desert, *J. Appl. Meteor.*, *13*, 863-870, 1974.

Shinn, E., G. Smith, J. Prospero, et al., African dust and the demise of Caribbean coral reefs, *Geophys. Res. Lett.*, *19*, 3029-3032, 2000.

Slinn, S. A., and W. G. N. Slinn, Predictions for particle deposition on natural waters, *Atmos. Environ.*, *14*, 1013-1016, 1980.

Wang, J., and S. A. Christopher, Intercomparison between satellite-derived aerosol optical thickness and PM2.5 mass: Implications for air quality studies, *Geophys. Res. Lett.*, *30*, doi:10.1029/2003GL018174, 2003.

Wang, J., S. A. Christopher, J. S. Reid, H. Maring, D. Savoie, B. H. Holben, J. M. Livingston, P. Russell, and S. K. Yang, GOES 8 retrieval of dust aerosol optical thickness over the Atlantic Ocean during PRIDE, *J. Geophys. Res.*, *108*, doi:10.1029/2002JD002494, 2003.

Wang, J., U. Nair, and S. Christopher, GOES-8 Aerosol Optical Thickness Assimilation in a Mesoscale Model: Online Integration of Aerosol Radiative Effects, *J. Geophys. Res.*, submitted, doi:2004JD004827, 2004.